

The Impact of Rotation on the Evolution of Low-Mass Stars

Daniel Brown and Maurizio Salaris

*Astrophysics Research Institute, JMU Liverpool, Twelve Quays House, Egerton Wharf, Birkenhead
CH41 1LD, UK,*

Abstract. High precision photometry and spectroscopy of low-mass stars reveal a variety of properties standard stellar evolution cannot predict. Rotation, an essential ingredient of stellar evolution, is a step towards resolving the discrepancy between model predictions and observations.

The first rotating stellar model, continuously tracing a low-mass star from the pre-main sequence onto the horizontal branch, is presented. The predicted luminosity functions of globular clusters and surface rotation velocities on the horizontal branch are discussed.

Keywords: Stellar rotation, Low-mass stars, HB stars, LF functions

PACS: 97.10.Kc

INTRODUCTION

We include rotation into the stellar evolution code FRANEC (Pietrinferni et al., 2004). The stellar structure equations were corrected for the effects of rotation according to the prescription given in Kippenhahn & Thomas (1970), allowing a 1D treatment of the stellar structure.

Additional to chemical element transport via convection and atomic diffusion, rotational mixing (described only by the shear instability) is introduced. The chemical element and angular momentum transport induced by rotational mixing is treated as a diffusive process with a diffusion coefficient given by Denissenkov & Weiss (2004). The change in the total angular momentum is accounted for during the entire evolution of the stellar model by disk braking (Pre-Main Sequence, PMS, see Shu et al. 1994), magnetic-wind braking (Main Sequence, MS, see Chaboyer et al. 1995), and mass loss (Red-Giant Branch, RGB).

CALIBRATION

Realistic initial conditions have to be found and free parameters have to be calibrated in order to predict the rotational properties of the stellar model and their effect on the evolution.

The initial angular rotation velocity ω_0 is chosen to reproduce the mean rotational period ($P_{1\text{Myr}}$) of 5 d derived from a sample of young PMS stars (Rebull 2001, Herbst et al. 2002, and Littlefair et al. 2005) in the mass range used for calibrating surface-rotation rates for the Hyades. To determine the initial rotation rates ω_0 for lower metallicities, the total angular momentum of stars of the same mass, but different metallicities, is as-

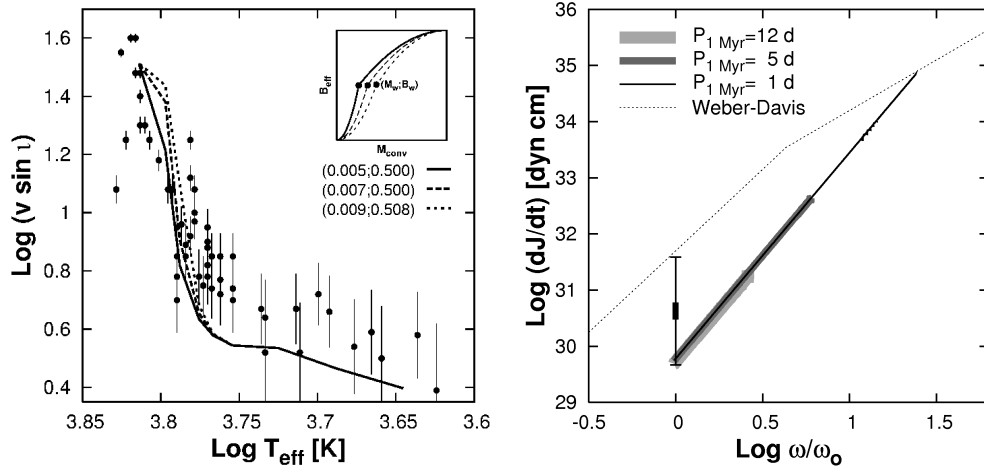


FIGURE 1. *Left:* The observed $\langle v \sin i \rangle$ in the Hyades from Soderblom et al. (1993) as a function of T_{eff} including a $\sim 1.3 \text{ km s}^{-1}$ error (Soderblom et al., 1993) as a function of $\log(T_{\text{eff}})$, derived from their (B–V) colours with the transformation relationship by Alonso et al. (1996). The profile of the B_{eff} functions describing the generation efficiency of magnetic fields in the magnetic–wind braking scenario are given in the inset, including the point $(M_w; B_w)$ that defines the shape of the B_{eff} function. Isochrones for $\langle v \sin i \rangle$ are shown using different B_{eff} functions: (0.005;0.500) solid, (0.007;0.500) long dashed, and (0.009;0.508) short–dashed line. The isochrone with (0.005;0.500) has the best χ^2 minimisation fit to the data and this B_{eff} function is chosen for the further work. *Right:* The rate of angular momentum loss ($\frac{dJ}{dt}$) by magnetic–wind braking is plotted against the angular surface rotation rate (ω). The rotational properties of the solar models with $\tau_{\text{DB}}=30 \text{ Myr}$, but three different initial angular velocities are shown: $\omega_0 = 4.064 \times 10^{-7} \text{ s}^{-1}$ ($P_{1 \text{ Myr}}=12 \text{ d}$ – light grey line), $\omega_0 = 9.740 \times 10^{-7} \text{ s}^{-1}$ ($P_{1 \text{ Myr}}=5 \text{ d}$ – grey line), and $\omega_0 = 4.870 \times 10^{-6} \text{ s}^{-1}$ ($P_{1 \text{ Myr}}=1 \text{ d}$ – black line). Observed $\frac{dJ}{dt}$ values for the Sun ($\log \frac{\omega}{\omega_0} = 0$) and a theoretically derived upper limit of a realistic 2D Weber–Davis solar–wind model (Weber & Davis, 1967) for the MS (dotted) is shown.

sumed to be the same at the start of their life as a PMS star. Disk braking ceases at a time $\tau_{\text{DB}} = 5 \text{ Myr}$ after which no significant amount of circum–stellar disks can be observed.

The free parameters linked to the mixing length and the magnetic–wind braking are calibrated comparing models with observed properties of the Sun (e.g. radius, luminosity, and surface rotation rate) and surface rotation rates observed for the Hyades (see left panel of Fig. 1). The influence of changes to the magnetic–wind braking prescription (e.g. the B_{eff} function, see inset on the left panel of Fig. 1) is also demonstrated by the solid, long–dashed, and short–dashed lines in the left panel of Fig. 1. The calibration of the braking processes is furthermore confirmed by comparing the rate of angular momentum loss of our models to the present Sun and an upper limit of a realistic 2D Weber–Davis solar–wind model (Weber & Davis, 1967) (see right panel of Fig. 2).

RESULTS

We aim to produce isochrones and Luminosity Functions (LFs) of globular clusters in the Galaxy in order to derive the impact of rotation with our realistic rotating stellar model to improve on prior exploratory work by Vandenberg et al. (1998). In addition,

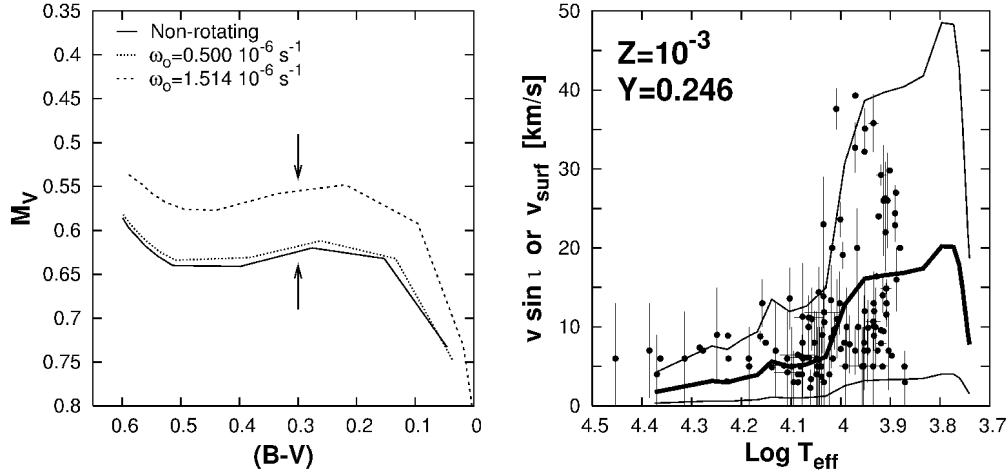


FIGURE 2. *Left:* The influence of rotation on the CMD of the ZAHB ($Z=10^{-3}$, $Y=0.246$) is presented for three predicted cases of non-rotating models (solid line), $\omega_0 = 0.5 \times 10^{-6} \text{ s}^{-1}$ (dotted line), and $\omega_0 = 1.514 \times 10^{-6} \text{ s}^{-1}$ (dashed line). The ZAHB including the effects of rotation ($\omega_0 = 1.514 \times 10^{-6} \text{ s}^{-1}$) has an increased brightness at $(B-V)=0.3$ mag (indicated by arrows) of $\Delta M_V = 0.07$ mag compared to the non-rotating case. *Right:* The predicted ZAHB surface rotation velocities given as a function of effective temperature for a chemical composition on the ZAHB of $Z=10^{-3}$, $Y=0.246$. The thick line represents values derived with the previously determined ω_0 . The thin lines mark the upper and lower limit of predicted ZAHB rotation values for initially faster or slower rotating stars, respectively. Observed HB data in M 15 (Behr et al. 2000 and Recio-Blanco et al. 2004), M 79 (Recio-Blanco et al., 2004), M 13 (Peterson et al. 1995 and Behr et al. 2000), NGC 2808 (Recio-Blanco et al., 2004), and M 80 (Recio-Blanco et al., 2004) is also included.

we predict the surface rotation velocity of Zero Age Horizontal Branch (ZAHB) stars. The recent increase in observed ZAHB rotation rates and our new rotating stellar model allow improvements to the theoretical work by Sills & Pinsonneault (2000). All models have a chemical composition of $Z=10^{-3}$ and $Y=0.246$, typical for globular clusters in the Galaxy (Zinn & West, 1984).

The Colour-Magnitude Diagram (CMD) of ZAHB is determined for varying ω_0 (non-rotating, $0.5 \times 10^{-6} \text{ s}^{-1}$, and $1.514 \times 10^{-6} \text{ s}^{-1}$), given in the left panel in Fig. 2. Rotation increases the ZAHB brightness, since faster rotating RGB stars develop a more massive helium core at the time of the helium flash.

ZAHB rotation rates are predicted using realistic initial conditions. A relationship on the ZAHB between the surface angular velocity, properties of the surface convective region, and the amount of angular momentum in the envelope around the helium core at the tip of the RGB is determined. It is important to note that the angular momentum within only the surface convective region determines the surface rotation rate of the ZAHB star. The relationship has been derived with the predicted ZAHB rotation rate of a $0.8 M_{\odot}$ model (without mass loss) that has been followed through the helium flash and then extended to hotter ZAHB stars. The predicted ZAHB rotation rates for a realistic range of ω_0 determined from the above mentioned sample of young PMS stars are compared with observations and given in the right panel of Fig. 2.

The impact of rotation on LFs was analysed with four stellar models (0.6, 0.7, 0.8,

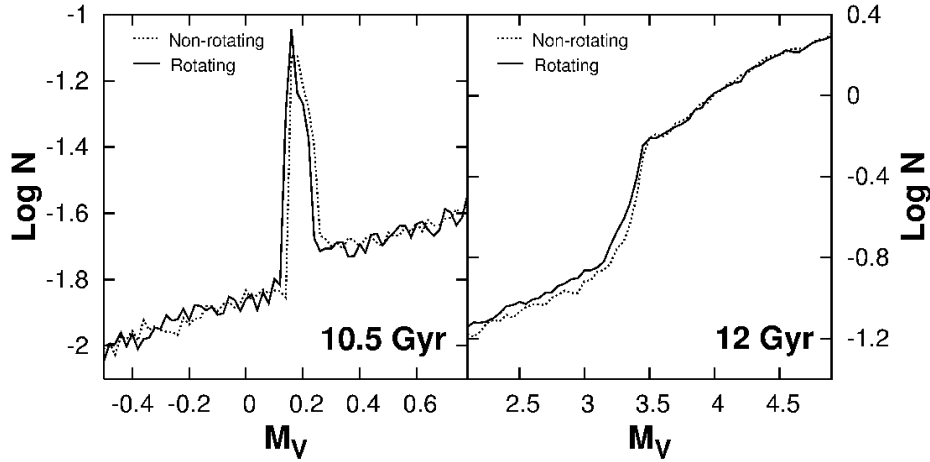


FIGURE 3. LFs for initial chemical composition of $Z=10^{-3}$, $Y=0.246$ are shown. *Left:* Two LFs of the RGB bump are shown for a 10.5 Gyr old isochrone. The first includes rotation ($\omega_0 = 1.514 \times 10^{-6} \text{ s}^{-1}$; solid line) and the second does not (dotted line). Rotation increases the brightness of the RGB bump by $\Delta M_V = 0.021$ mag. *Right:* 12 Gyr old LFs are shown. The LF including rotation is plotted as solid lines and the non-rotating comparison is plotted as a dotted line. The SGB shows a less steep change in the LF when rotation is included, leading to a 11 % increase in number of stars at the base of the RGB.

and $0.85 M_\odot$) from which two LFs were generated (10.5 Gyr and 12 Gyr). The young LF demonstrates that rotation increases the brightness of the RGB bump by 0.021 mag (see left panel in Fig. 3). This increase is within the scatter of the brightness difference Δ_{HB}^{bump} between RGB bump and HB for this metallicity (Riello et al., 2003). The old LF illustrates how rotation reduces the Sub Giant Branch (SGB) slope and increases the number of stars at the base of the RGB by 11 % (right in Fig. 3). The increase in the number count at the base of the RGB is still detectable (5 %) when comparing the non-rotating 12 Gyr old and rotating 10.5 Gyr old LF, where both cases are in agreement with observational constraints.

SUMMARY

The rotating models demonstrate the brightening of the ZAHB and RGB bump due to rotation. A $\omega_0 = 1.514 \times 10^{-6} \text{ s}^{-1}$ results in an increased brightness of the ZAHB of $\Delta M_V = 0.07$ mag and an increased brightness of the RGB bump of $\Delta M_V = 0.021$ mag compared to the non-rotating case. The increase in the helium-core mass and number count at the base of the RGB are just two effects of stellar rotation on low-mass stars that will be addressed in future work.

The rotating code and its capability to follow the evolution through the helium flash makes it the first stellar evolution code to include rotation during the helium-flash phase for low-mass stars. Given realistic initial rotation rates, the code allows us to predict the ZAHB velocity distribution. These predicted rotation rates agree better with observations than rates determined in the most recent theoretical work by Sills & Pinsonneault

(2000). Our determined ZAHB surface rotation rates explain the apparent “bimodality” of the rotation rates at 11 000 K (see right panel in Fig. 2) without the need of a bimodality in the initial rotation rates and its survival up to the tip of the RGB.

REFERENCES

- Alonso A., Arribas S., Martínez-Roger C., 1996, *Astronomy & Astrophysics*, 313, 873
Behr B. B., Cohen J. G., McCarthy J. K., 2000, *Astrophysical Journal*, 531, L37
Behr B. B., Djorgovski S. G., Cohen J. G., McCarthy J. K., Cote P., Piotto G., Zoccali M., 2000, *Astrophysical Journal*, 528, 849
Chaboyer B., Demarque P., Pinsonneault M. H., 1995, *Astrophysical Journal*, 441, 876
Denissenkov P. A., Weiss A., 2004, *Astrophysical Journal*, 603, 119
Herbst W., Bailer-Jones C. A. L., Mundt R., Meisenheimer K., Wackermann R., 2002, *Astronomy & Astrophysics*, 396, 513
Kippenhahn R., Thomas H. C., 1970, *Stellar Rotation*. A. Slettebak
Littlefair S. P., Naylor T., Burningham B., Jeffries R. D., 2005, *Monthly Notices of the Royal Astronomical Society*, 358, 341
Peterson R. C., Rood R. T., Crocker D. A., 1995, *Astrophysical Journal*, 453, 214
Pietrinferni A., Cassisi S., Salaris M., Castelli F., 2004, *Astrophysical Journal*, 612, 168
Rebull L. M., 2001, *Astronomical Journal*, 121, 1676
Recio-Blanco A., Piotto G., Aparicio A., Renzini A., 2004, *Astronomy & Astrophysics*, 417, 597
Riello M., Cassisi S., Piotto G., Recio-Blanco A., De Angeli F., Salaris M., Pietrinferni A., Bono G., Zoccali M., 2003, *Astronomy & Astrophysics*, 410, 553
Shu F., Najita J., Ostriker E., Wilkin F., 1994, *Astronomical Journal*, 429, 781
Sills A., Pinsonneault M. H., 2000, *Astrophysical Journal*, 540, 489
Soderblom D. R., Stauffer J. R., Hudon J. D., Jones B. F., 1993, *Astrophysical Journal Supplement Series*, 85, 315
Vandenberg D. A., Larson A. M., De Propris R., 1998, *Astronomical Society of the Pacific*, 110, 98
Weber E. J., Davis L., 1967, *Astrophysical Journal*, 148, 217
Zinn R., West M. J., 1984, *Astrophysical Journal Supplement Series*, 55, 45

